Transient Discharge of Solid Particles from Upper Outlet of Vertical Bubble Columns

Nobuyuki Hidaka, Kazuhiro Kakoi, and Toshitatsu Matsumoto
Dept. of Applied Chemistry and Chemical Engineering, Kagoshima University, Kogashima 890, Japan

Shigeharu Morooka
Dept. of Chemical Science and Technology, Kyushu University, Fukuoka 812, Japan

Sieved glass beads of 230, 280 and 470 μm dia. were steadily suspended by upward concurrent gas and liquid flows in vertical bubble columns of 7 cm dia. and 4.85 m height or 15 cm dia. and 2.7 m height. Then the liquid velocity was suddenly increased to a higher value, which caused an unsteady-state discharge of solid particles from the top of the column. The transient discharge rate was determined by collecting solid particles in the effluent, and transient axial distributions of gas and solid holdups along the column length were measured by sectioning the column with horizontal shutter plates just after stopping gas and liquid flows. A 1-D sedimentation-dispersion model was applied to describe the unsteady-state discharge rate of solid particles as well as the change in gas and solid holdups in the columns. The model developed successfully expressed the transient behavior of solid particles over entire columns consisting of dense and dilute regions.

Introduction

Three-phase fluidization is an important technique for contacting gas, liquid, and solid particles and is widely used in petroleum and biochemical processes. Many works (Imafuku et al., 1968; Kato et al., 1972, 1985; Smith and Ruether, 1985; Morooka et al., 1986; Smith et al., 1986; Murray and Fan, 1989; Matsumoto et al., 1989, 1991, 1992; Hidaka et al., 1992) have been published on the behavior of solid particles in columns. Fan (1989) summarized results on fundamentals and applications of three-phase fluidization up to 1989. However, most of the previous studies were limited to cases of steady-state operations. Very little information is available on the transient behavior of three-phase columns.

Jiřicný and Stanék (1990) investigated transient behavior of countercurrent air–water flow in a packed bed. They simulated unsteady-state dynamics after a step change in gas and liquid velocities, using a first-order kinetics model. Hidaka et al. (1993) investigated transient responses of axial distributions of gas and solid holdups in a bubble column with suspended solid particles. They operated the column batchwise with respect to solid particles and decreased or increased the liquid velocity. When the liquid velocity was increased, the decrease of solid holdup in the bottom region was compensated by an increase in the freeboard region. The new steady state was obtained in a time period of the order of 1 min. The transient behavior of solid particles, which were not discharged from the outlet in their experiment, was well-described by a one-dimensional sedimentation-dispersion model over an entire column. Experience often shows, however, that most of solid particles are abruptly entrained when the liquid velocity is increased, even if the new liquid velocity is smaller than the terminal velocity of the solid particles in an isolated condition. This causes a serious problem at the startup of three-phase fluidized beds, but no principle has been reported for controlling the transient behavior of solid particles.

In this study, sieved glass beads are fluidized in vertical columns of 7 cm and 15 cm dia., and an unsteady-state discharge of solid particles from the upper outlet is induced by a step increase in liquid velocity. The time-dependent discharge rate of particles and the axial distributions of gas and solid holdups in columns are determined experimentally and simulated with an unsteady-state sedimentation-dispersion model.

Correspondence concerning this article should be addressed to T. Matsumoto.

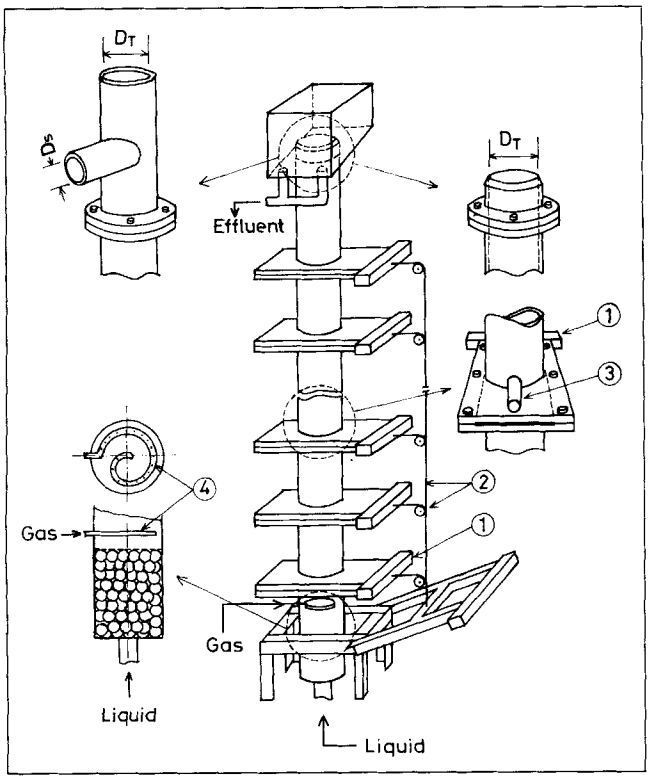

Figure 1. Experimental apparatus.

(1) Shutter plate; (2) wire and pulley; (3) withdrawal tap; (4) gas distributor.

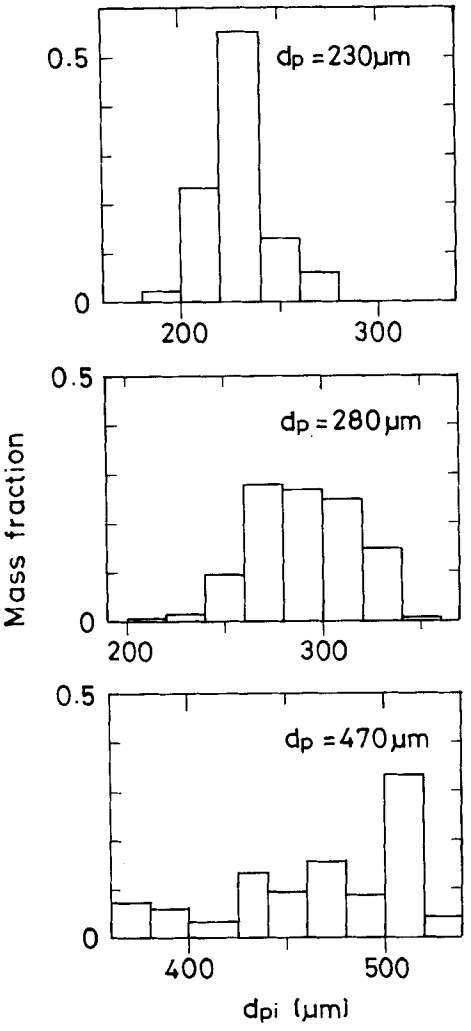

Figure 2. Size distributions of glass beads used.

Experimental Apparatus and Procedure

Figure 1 is a diagram of the experimental setup. The three-phase fluidization column, made of a 7-cm-ID, 4.25-m-high acrylic resin pipe was set vertically. The top end of the column was fabricated as a sharp edge. To evaluate the effect of the exit configuration on the discharge rate of solid particles, the outlet was changed to a tube of 10 cm length fixed horizontally at a height of 4.25 m from the bottom. The diameter of the side tube, d_s, was 1.2, 3.0 and 7.0 cm. The local solid holdup in the column was determined by twenty shutter plates, made of 3-mm-thick stainless steel and installed horizontally at 0.2 m intervals. The shutter plates were interconnected with a wire rope and sectioned the column instantly. The gas tightness was assured with O-rings. The column, 15 cm in diameter and 2.7 m in height, was equipped with eleven shutter plates, and the other features were fundamentally the same as those of the 7-cm-diameter column. The gas distributor and other details have been described elsewhere (Matsumoto et al., 1989, 1991, 1992).

Air and tap water were used, respectively, as the gas and liquid phases. The liquid temperature was about 20°C. The solid phase was sieved glass beads. Their properties and size distributions are, respectively, shown in Table 1 and Figure 2. After the bed was continuously operated for 0.5 h batchwise with respect to solid particles, the liquid velocity was momentarily increased, at which point the discharge of particles from top of the column began. Solid particles in the effluent were collected, dried, and weighed. Local values of gas and solid holdups were measured by stopping the flows and closing the shutters simultaneously (Al-Dibouni and Garside, 1979; Matsumoto et al., 1992; Hidaka et al., 1992). The solid holdup was defined as the volume fraction of particles suspended in a unit volume of slurry. Measurements of solids discharge and local phase holdups were performed repeatedly at prescribed elapsed times under the same flow conditions. The mean gas holdup was calculated from the total volume of gas in each section.

Experimental Results

Figure 3A shows transient changes in the solid holdup, ϕ_p, when 470-μm-dia. particles were fluidized in the 7-cm-dia. column. The liquid velocity was increased from $U_{11} = 0.027$

Table 1. Properties of Glass Beads and Parameters

d_p [μm]	ρ_p [Mg/m^3]	v_t [m/s]	Ga	n, Eq. 26
230	2.5	0.026	179	2.93
280	2.5	0.034	323	2.75
470	2.5	0.067	1,526	2.40

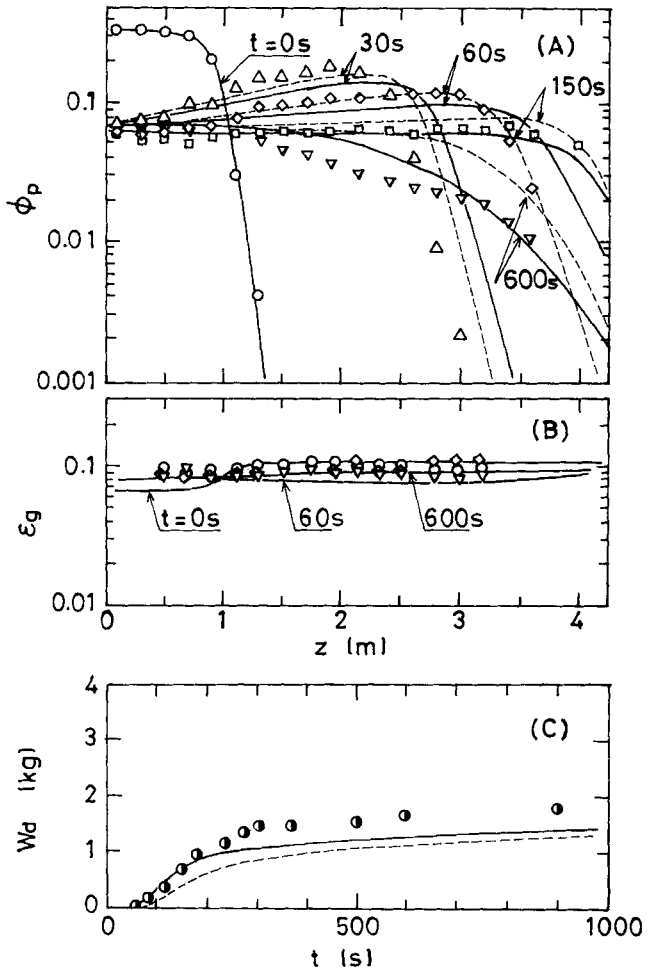

Figure 3. Transient changes in flow properties.

Solid and broken lines are calculated by assuming nine- and single-component particles, respectively. (A) Axial distribution of solid holdup; (B) axial distribution of gas holdup; (C) accumulated mass of solid particles discharged. Experimental conditions: $D_T = 0.07$ m; $d_p = 470$ μm; $W_{c1} = 3.0$ kg; $\epsilon_g = 0.1$; $U_g = 0.043$ m/s; $U_{11} = 0.027$ m/s; $U_{12} = 0.08$ m/s. Elapsed time: ○, 0 s; △, 30 s; ◇, 60 s; □, 150 s; ▽, 600 s.

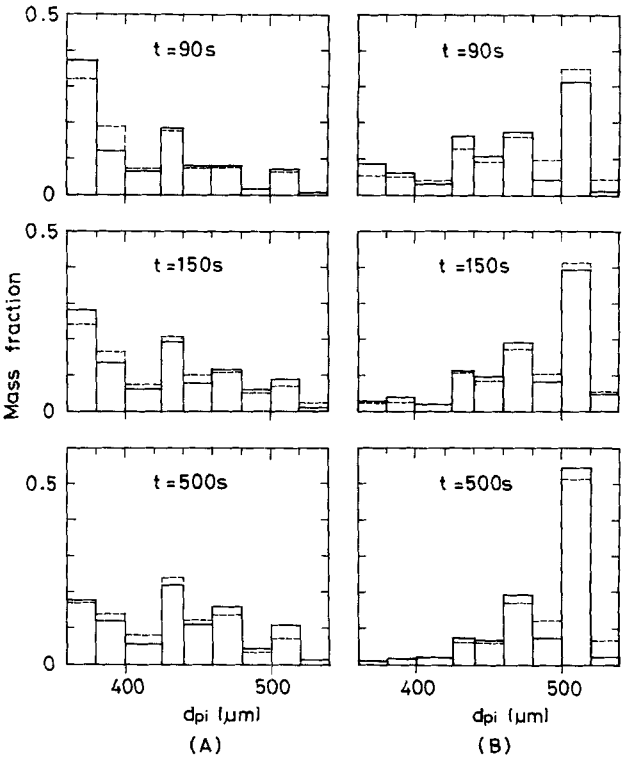

Figure 4. Transient change in size distribution of solid particles.

Experimental conditions are the same as in Figure 3. (A) Solid particles discharged; (B) solid particles left in column. Solid and broken lines are experimental and calculated results, respectively.

m/s to $U_{12} = 0.08$ m/s at a fixed gas velocity of $U_g = 0.043$ m/s. As indicated in Figure 3B, the average gas holdup, ϵ_g, before the change was 0.1. The solid holdup at the bottom of the column decreased quickly, and a maximum solid holdup zone appeared. This zone gradually moved upward and disappeared at 600 s. The solid holdup at the top of the column increased, and the discharge from the outlet began at about 50 s after the change in liquid velocity. Figure 3C indicates that the accumulated amount of discharged solid particles approached a constant value. This means that the discharge rate of solid particles became asymptotically zero. The time-averaged linear velocity of i particles with respect to the fixed coordinate at an axial position z is written as

$$u_{pi} = u_1 - u_{ti} = U_1/[(1-\epsilon_g)(1-\phi_{pi})] - u_{ti}, \qquad (1)$$

where u_{ti} is the settling velocity of i particles in a quiescent fluid, and u_1 is the linear velocity of liquid. If u_{pi} is positive for all particles, the solid holdup finally reaches zero. In the run of Figure 3, however, u_{pi} was negative in spite of the increase in the liquid velocity. Thus a new steady state was established, where the average holdup was smaller than that at the initial liquid velocity. Figure 3B reveals that the gas holdup became constant through the column after the dense zone of $\phi_p = 0.33$ vanished.

Figure 4 shows time-dependent changes in the size distribution of solid particles that were collected in the effluent or sampled from the bottom of the column. The experimental conditions were the same as in Figure 3. At $t = 500$ s, particles smaller than 410 μm were rarely found at the column's bottom.

Figures 5A, 5B and 5C show transient responses at $U_g = 0.21$ m/s and $\epsilon_g = 0.3$ in the 0.07-cm-dia. column, and Figures 6A, 6B and 6C show these responses at $U_g = 0.054$ m/s and $\epsilon_g = 0.1$ in the 15-cm-dia. column. The average particle size was 470 μm, and the liquid velocity was increased from about 0.03 m/s to about 0.08 m/s. As in Figure 3, the discharge of solid particles was initiated by the change in liquid velocity. The wave of a maximal solid holdup seen at $t = 30$ and 90 s in the 7-cm-dia. column was not observed in the 15-cm-dia. column. A larger axial dispersion in the larger column scattered the local maximal solid holdup in an early transient stage.

Modeling for Transient Behavior of Solid Holdup with Discharge of Solid Particles

A solid particle reaches its terminal velocity within roughly 0.1 s under the conditions of the present study (Hidaka et al.,

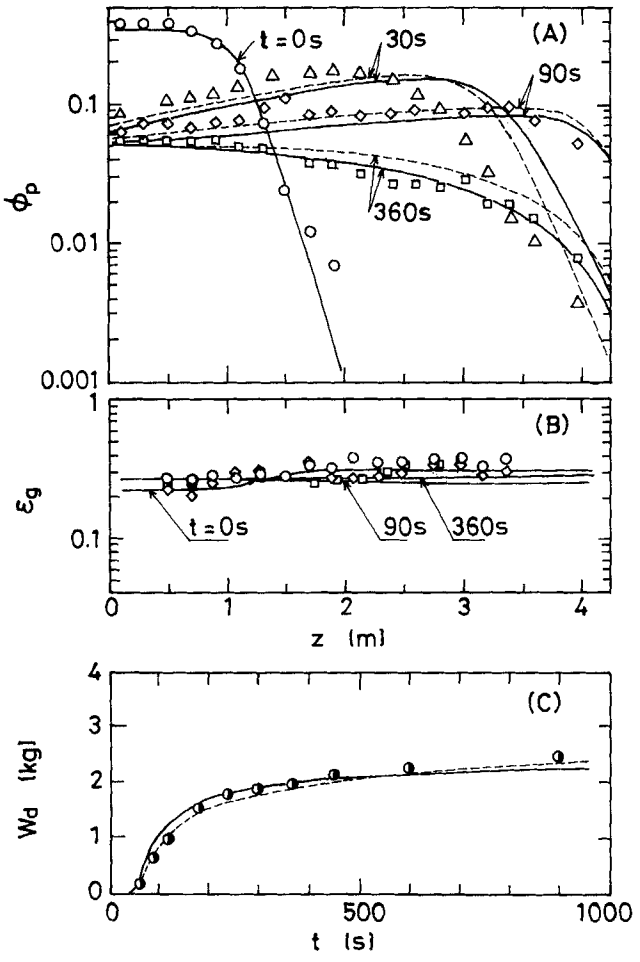

Figure 5. Transient changes in flow properties.

Solid and broken lines are calculated by assuming nine- and single-component particles, respectively. (A) Axial distribution of solid holdup; (B) axial distribution of gas holdup; (C) accumulated mass of solid particles discharged. Experimental conditions: $D_T = 0.07$ m; $d_p = 470$ μm; $W_{c1} = 3.0$ kg; $\epsilon_g = 0.3$; $U_g = 0.21$ m/s; $U_{l1} = 0.027$ m/s; $U_{l2} = 0.080$ m/s. Elapsed time: ○, 0 s; △, 30 s; ◇, 90 s; □, 360 s.

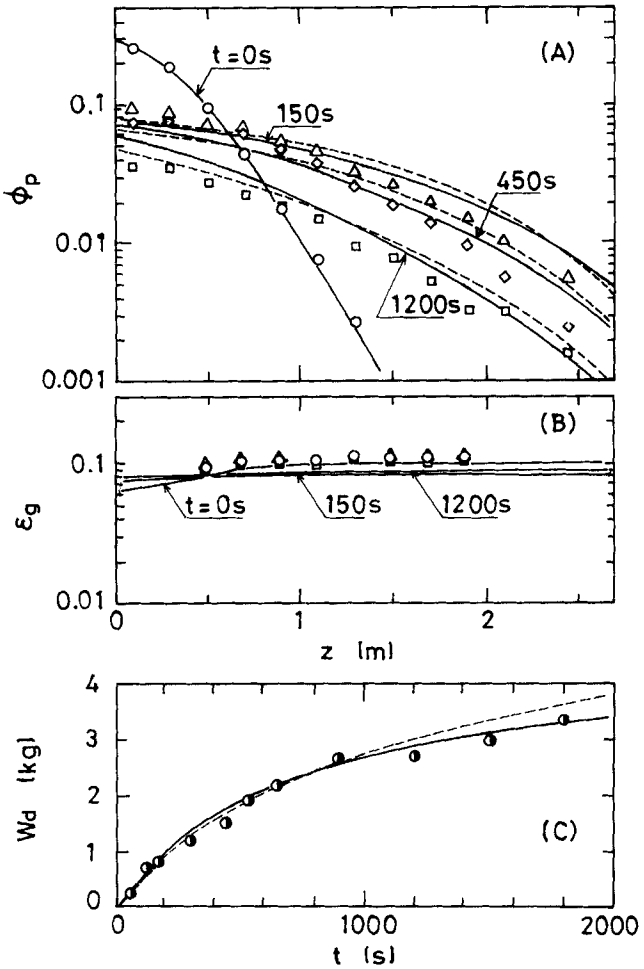

Figure 6. Transient changes in flow properties.

Solid and broken lines are calculated by assuming nine- and single-component particles, respectively. (A) Axial distribution of solid holdup; (B) axial distribution of gas holdup; (C) accumulated mass of solid particles discharged. Experimental conditions: $D_T = 0.15$ m; $d_p = 470$ μm; $W_{c1} = 5.0$ kg; $\epsilon_g = 0.1$; $U_g = 0.054$ m/s; $U_{l1} = 0.029$ m/s; $U_{l2} = 0.075$ m/s. Elapsed time: ○, 0 s; △, 150 s; ◇, 450 s; □, 1,200 s.

1993). This time period is very short compared with that in which the axial solid holdup settles after a step change in the liquid velocity. Therefore, the local motion of solid particles is of quasi-steady state and can be described only by the following unsteady-state material balance, neglecting the equation of motion (Matsumoto et al., 1992; Hidaka et al., 1993):

$$\frac{\partial \phi_{pi}}{\partial t} + \frac{\partial}{\partial z}\left[u_{pi}\phi_{pi} - E_{pi}\frac{\partial \phi_{pi}}{\partial z}\right] = 0, \tag{2}$$

where ϕ_{pi} is the solid holdup of i particles at t and z. The initial condition of Eq. 2 is

$$t < 0; \quad \phi_{pi}(0,z) = \phi_{pi0}(z), \tag{3}$$

where $\phi_{pi0}(z)$ is the steady-state axial distribution before the liquid velocity is changed. Since there is no flow due to dispersion across the inlet boundary, the boundary condition is expressed by

$$z = 0; \quad u_{pi}\phi_{pi} - E_{pi}\frac{\partial \phi_{pi}}{\partial z} = 0. \tag{4}$$

At the top of the column, solid particles are entrained by the liquid flow moving laterally, and some of them return to the column due to gravity. Thus the solid concentration in the effluent flow, $\phi_{pi}|_{z=H+0}$, is always lower than that just inside the column, $\phi_{pi}|_{z=H-0}$. The returning rate of solid particles is decided by the dynamic balance between the carriage by the radial liquid flow and the fall by gravity. Figure 7 illustrates the model of the overflow at the exit. The three-phase mixture expands above the column end to a thickness h and flows radially. If there is no vertical change in the radial flow layer, the radial liquid velocity at the column rim, U_{lr}, is related to the vertical liquid velocity in the column, U_l, as follows:

$$\pi D_T h U_{lr} = (\pi D_T^2/4)U_l \tag{5}$$

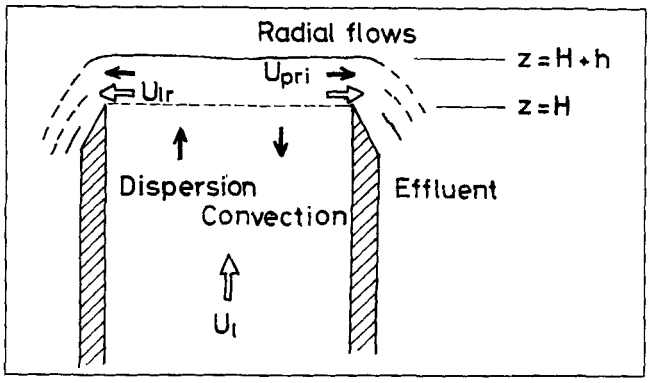

Figure 7. Overflow at column exit.

The mass of solid particles transferred by the dispersion into the boundary zone from the column is $(\pi D_T^2/4)(1-\epsilon_g)E_{pi}\partial\phi_{pi}/\partial z|_{z=H-0}$, and that returned to the column by the convective flow is $(\pi D_T^2/4)(1-\epsilon_g)u_{pi}\phi_{pi}|_{z=H-0}$, if the solid holdup in the boundary zone at a given time is constant at any position. The mass of the solid particles entrained in the effluent flow is expressed as $\pi D_T h U_{pri}\phi_{pi}|_{z=H+0}$, where U_{pri} is the radial velocity of the solid phase at the column rim. Then the material balance of i particles at $z=H$ is given as as

$$\frac{\pi D_T^2}{4}(1-\epsilon_g)\left[u_{pi}\phi_{pi}-E_{pi}\frac{\partial\phi_{pi}}{\partial z}\right]_{|z=H-0} = \pi D_T h U_{pri}\phi_{pi}|_{z=H+0}. \quad (6)$$

From Eqs. 5 and 6, the boundary condition at the outlet is

$$z=H; \quad \left[u_{pi}\phi_{pi}-E_{pi}\frac{\partial\phi_{pi}}{\partial z}\right]_{|z=H-0} = K_{pri}\phi_{pi}|_{z=H+0} \quad (7)$$

where K_{pri} is given as follows:

$$K_{pri}=\frac{U_1}{1-\epsilon_g}\frac{U_{pri}}{U_{1r}}. \quad (8)$$

In the heterogeneous bubble-flow regime, gas and liquid phases are well mixed in the boundary zone of $z=H\sim H+h$. Then we can assume that U_{pri} is mostly decided by the turbulence at the column rim and is little dependent on the terminal velocity of each particle:

$$K_{pri}=K_{pr} \quad (9)$$

which should be determined experimentally.

For an unsteady-state operation, the boundary condition at the exit, Eq. 7, is indispensable. For a steady-state operation, however, only one boundary condition is necessary (Kato et al., 1972; Smith and Ruether, 1985); K_{pr} should be given as an experimental term.

Determination of K_{pr}. Integrating Eq. 2 from $z=0$ to $z=H-0$, we obtain

$$\frac{\partial}{\partial t}\int_0^H \phi_{pi}\ dz+\left[u_{pi}\phi_{pi}-E_{pi}\frac{\partial\phi_{pi}}{\partial z}\right]_{|z=H-0} - \left[u_{pi}\phi_{pi}-E_{pi}\frac{\partial\phi_{pi}}{\partial z}\right]_{|z=0}=0. \quad (10)$$

The second term is equal to $K_{pr}\phi_{pi}|_{z=H+0}$ from Eq. 7, and the third term is zero from Eq. 4. Then we get

$$-\frac{\partial}{\partial t}\int_0^H \phi_{pi}\ dz = K_{pr}\phi_{pi}|_{z=H+0}. \quad (11)$$

The value of $\int_0^H \phi_{pi}\ dz$ is calculated from the mass balance of i particles:

$$\int_0^H \phi_{pi}\ dz=\frac{W_{ci}}{(\pi D_T^2/4)(1-\epsilon_g)\rho_p}, \quad (12)$$

where W_{ci} is the mass of i particles existing in the column at time, t. The local solid holdup for all particles of $i=1\sim N$, shown in Figures 3A, 5A, and 6A, is calculated by accumulating ϕ_{pi} for each size section:

$$\phi_p=\sum_{i=1}^{N}\phi_{pi}. \quad (13)$$

The total mass of discharged particles for all components of $i=1\sim N$, indicated in Figures 3C, 5C, and 6C, is given by

$$W_d=\sum_{i=1}^{N}W_{di}=(\pi D_T^2/4)\rho_p\sum_{i=1}^{N}\int_0^t K_{pr}(1-\epsilon_g)\phi_{pi}|_{z=H+0}\ dt. \quad (14)$$

Figure 8 shows $\int_0^H \phi_p\ dz$ and $\phi_p|_{z=H-0}$ as functions of the elapsed time under the same experimental conditions as in Figure 3. The value of $\phi_p|_{z=H-0}$ was obtained by extrapolating the axial distribution of solid holdup to $z=H$ at a given elapsed time, and that of $K_{pr}\phi_p|_{z=H+0}$ was obtained by differentiating $\int_0^H \phi_p\ dz$, which was calculated from Eq. 12, with respect to time. Figure 9 shows the relationship between $K_{pr}\phi_p|_{z=H+0}$ and $\phi_p|_{z=H-0}$. The data are well correlated with the straight lines. From the gradient of each line, K_{pr} is obtained. Figure 10 shows that K_{pr} increases with increasing U_1 and ϵ_g, and is independent of column diameter and particle size. Thus the following equation was obtained experimentally.

$$K_{pr}=\frac{U_1}{(1-\epsilon_g)}\frac{1}{3(1-\epsilon_g)}\frac{\phi_p|_{z=H-0}}{\phi_p|_{z=H+0}}. \quad (15)$$

Numerical Calculation. Equations 2–4 and 7 were transformed into the dimensionless forms by using the following variables.

$$T=tU_1/H, \quad Z=z/H, \quad u_{pi}^*=u_{pi}/U_1, \quad E_{pi}^*=E_{pi}/(U_1H). \quad (16)$$

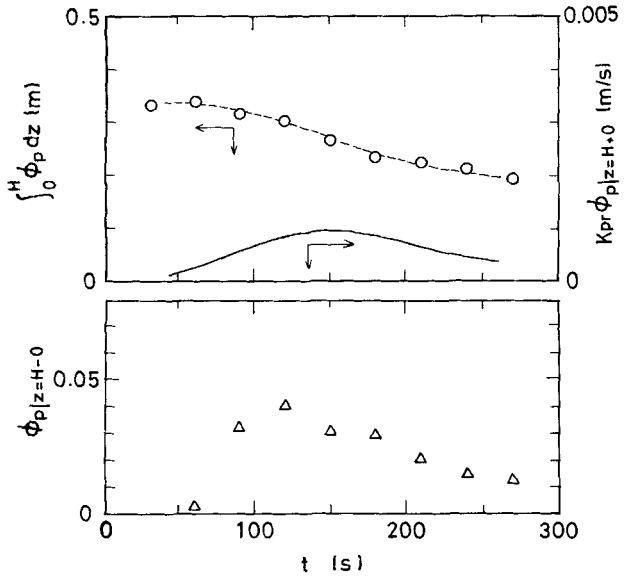

Figure 8. Transient changes in $\int_0^H \phi_p\, dz$, $K_{pr}\phi_p|_{z=H+0}$ and $\phi_p|_{z=H-0}$.

Experimental conditions are the same as in Figure 3.

Then the equations were rewritten in finite difference form, in which the upwind-difference approximation (Gosman et al., 1969) was applied to the convection term in Eq. 2. Next, a set of derived nonlinear tridiagonal equations was solved numerically. In the present computation, grid sizes were fixed as $\Delta Z = 0.025$ and $\Delta T = U_1/H$. The convergence criterion at each grid point was given as $(\phi_p^{j+1} - \phi_p^j)/\phi_p^j < 0.01$. The boundary condition at the exit was given by substituting Eq. 15 for K_{pri} in Eq. 7, regardless of d_{pi}, as discussed earlier. Unsteady-state solid holdup and discharged mass were thus obtained for i-component particles.

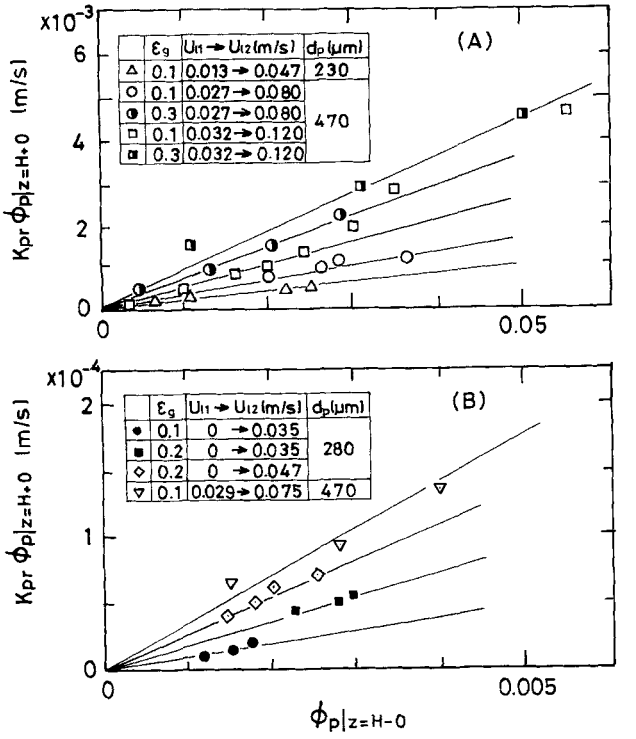

Figure 9. Relationship between $K_{pr}\phi_p|_{z=H+0}$ and $\phi_p|_{z=H-0}$.

(A) $D_T = 0.07$ m; (B) $D_T = 0.15$ m.

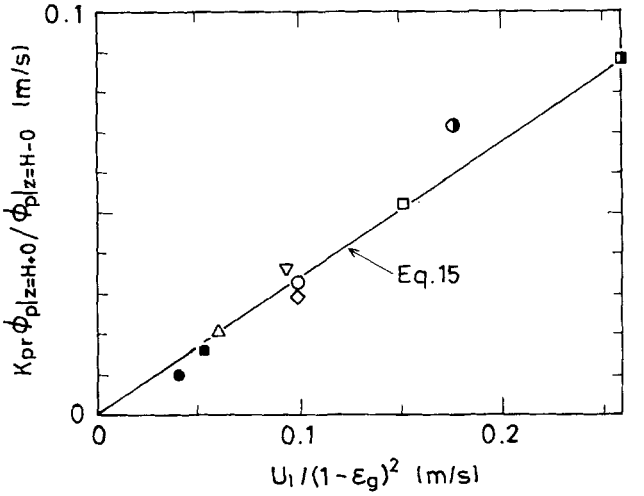

Figure 10. Correlation of K_{pr}.

Keys are the same as in Figure 9.

The parameters used in the model calculation have been correlated by Matsumoto et al. (1992) as follows.

(a) Local gas holdup for a gas–liquid–solid systems:

$$\epsilon_g = U_g(1-R)/\left\{0.29\left[1+2.5\phi_{pt}^{0.85}\right] + c_1 U_g(1-R)\right\}, \quad (17)$$

where $R = \epsilon_g U_1/[(1-\epsilon_g)U_g]$. The constant c_1 in Eq. 17 is 1.8 for $D_T = 0.07$ m and 2.4 for $D_T = 0.15$ m. The solid lines of the gas holdup shown in Figures 3, 5, and 6 are calculated from Eq. 17.

(b) Axial dispersion coefficient of i particles:

$$E_{pi} = \sum_{i=1}^{N} E_{pi0}\phi_{pi}/\phi_{pt}, \quad (18)$$

where the contribution of different components is accounted for by the volume fraction of each monocomponent. The axial dispersion of i particles alone, E_{pi0}, is related to the axial dispersion coefficient of liquid for the air–water system, E_1, by the following equation:

$$E_{pi0}/E_1 = 1 - 0.01\, Re_i^{*2/3}. \quad (19)$$

Equation 19 is valid for $Re_i^* = d_{pi}[\epsilon_g(1-R)(gD_T/2)]^{1/2}/\nu < 500$. The axial dispersion coefficient of liquid is expressed by

$$\frac{E_1}{(gD_T^3)^{1/2}} = \left\{\left[\frac{k[\epsilon_g(1-R)]^{1/2}}{1-\epsilon_g}\right]^3 + 0.09^3\right\}^{1/3} \quad (20)$$

for $D_T = 0.07$ m, $k = 0.3[1 + 4U_1/(1-\epsilon_g)]$; for $D_T = 0.15$ m, $k = 0.3$.

(c) Slip velocity between i particles and liquid velocity:

$$d_{pi}u_{ti}/\nu = Re_{ti} = Re_{\infty i} f_i \tag{21}$$

where Re_{∞_i} is defined by $v_{\infty_i} d_{pi}/\nu$, based on the settling velocity of isolated i particles, v_{∞_i}. According to Matsumoto et al. (1989, 1992), Re_{∞_i} is given by

$$Re_{\infty i} = \frac{Ga_i \zeta_i}{\left[18^{4/5} + (Ga_i \zeta_i/3.0)^{2/5}\right]^{5/4}}, \tag{22}$$

where

$$\zeta_i = 1 + \left\{ \frac{6.5[\epsilon_g(1-R)]^{1/2} Ga_i^{1/3}}{1 + \left\{[\epsilon_g(1-R)]^{1/2} Ga_i^{1/3}/15\right\}^2} \right\}^{3/2} Ga_i^{-2/3}. \tag{23}$$

The value of v_{∞_i} calculated from Eqs. 22 and 23 was nearly equal to the following equation, which was obtained in three-phase flow at very dilute solid concentrations (Morooka et al., 1986):

$$u_{ti}/v_{ti} = 1 + 10\epsilon_g (d_{pi} v_{ti}/\nu)^{-0.25} \tag{24}$$

In three-phase fluidized beds, the voidage function of Richardson and Zaki (1954) cannot be applied (Matsumoto et al., 1989), and the following equation for voidage function, f_i, for multicomponent systems has been obtained (Matsumoto et al., 1992):

$$f_i = \left\{(1-\phi_{pt})\left[1-(\phi_{pt}/\phi_{pc})^3\right]^{1/3}\right\}^{n_i - 1} \times \prod_{j=1}^{N} \left\{(1-\phi_{pj})\left[1-(\phi_{pj}/\phi_{pc})^3\right]^{1/3}\right\}^{n_j - n_i}, \tag{25}$$

where ϕ_{pc} is a correction factor equal to 0.55. The exponent in Eq. 25 for three-phase systems, n_i, is correlated by the following equation (Matsumoto et al., 1989, 1992).

$$(n_i - 2)/(5 - n_i) = 6.0\, Ga_i^{-1/2}. \tag{26}$$

Equations 17–26 have been verified with experimental data in three-phase fluidized beds for air–water–glass beads systems under these conditions (Matsumoto et al., 1992; Hidaka et al., 1993): column diameter, 7–15 cm; column length, 2.7–4.85 m; particle size, 66–540 μm; superficial gas velocity, 0.02–0.35 m/s; superficial liquid velocity, 0–0.15 m/s. The effects of particle density and concentration are expressed by Eqs. 22 and 23 and Eqs. 25 and 26, respectively. The flow behavior at a steady state at $t = 0$ and $U_1 = U_{11}$ are calculated by the procedure reported by Matsumoto et al. (1992), as functions of column dimensions and physical properties of liquid and solid particles.

Discussion

Glass beads with an average diameter of $d_p = 470$ μm were divided into nine components ($i = 9$), as shown in Figure 2. The solid lines in Figures 3, 5, and 6 indicate the calculated transient behavior with division into nine components. The broken lines show the results, assuming a single component ($d_p = 470$ μm). The calculation with the nine components is better than that with the single component. The differences between the solid and broken lines are small because the particle-size distribution was narrow, as indicated in Figure 2. The broken lines in Figure 4 show the calculated size distributions of solid particles in the column as well as the effluent flow at various elapsed times. The calculated and measured size distributions agree well.

Figure 11 reveals transitional changes in the mass of discharged particles measured in the 7-cm-dia. column, and Figure 12 shows these changes in the 15-cm-dia. column, respectively. The solid lines are calculated from Eq. 14, with parameters correlated by Eqs. 17–26, and are in agreement with the data. As indicated in Figure 13, the accumulated mass of discharged particles is expressed well by the present model.

The ratio of solid holdup at the exit, $\phi_{pi}|_{z=H+0}/\phi_{pi}|_{z=H-0}$, should be discussed further. Kato et al. (1972) described the axial distribution of solid holdup for a steady-state condition as

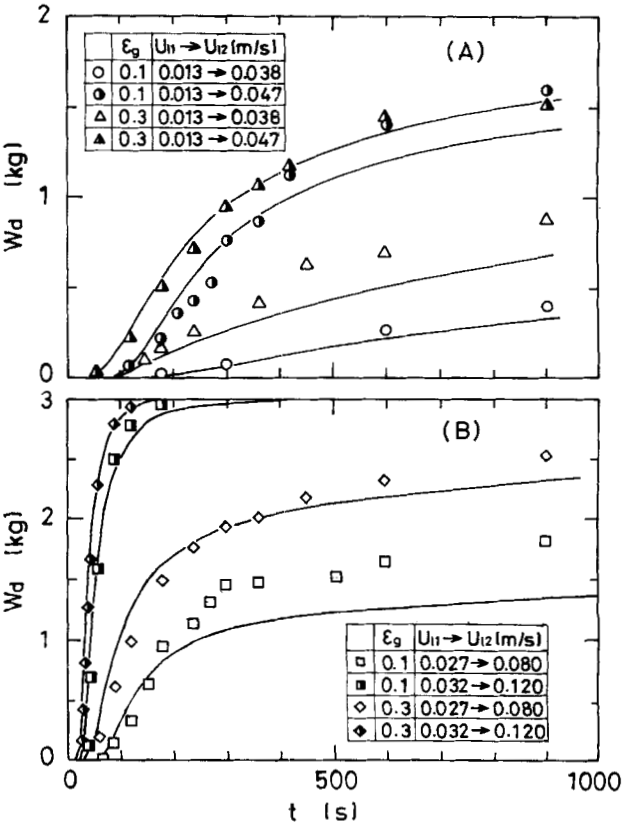

Figure 11. Accumulated mass of solid particles discharged from 7-cm-dia. column.

(A) $d_p = 230$ μm, $W_{c1} = 2.0$ kg; (B) $d_p = 470$ μm, $W_{c1} = 3.0$ kg.

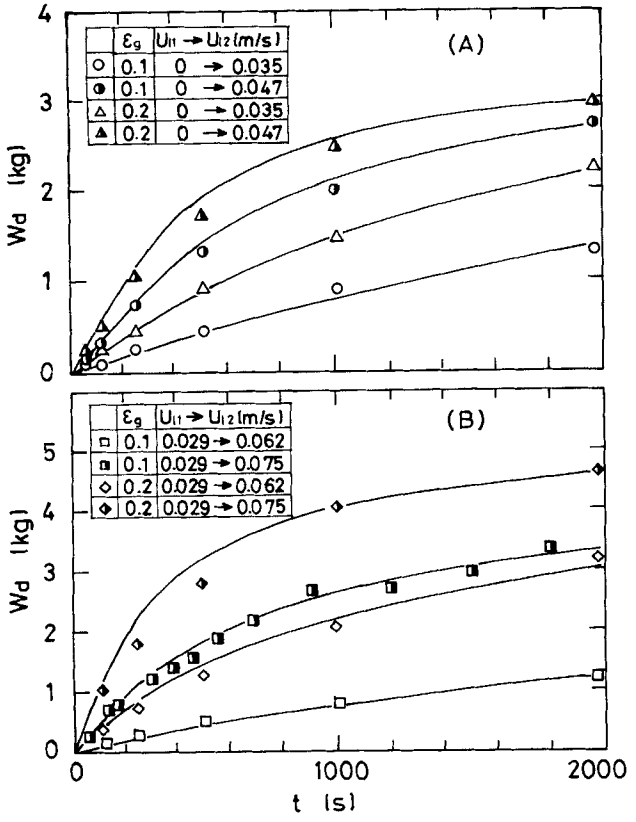

Figure 12. Accumulated mass of solid particles discharged from 15-cm-dia. column.

(A) $d_p = 280$ μm, $W_{c1} = 3.0$ kg; (B) $d_p = 470$ μm, $W_{c1} = 5.0$ kg.

$$u_p \phi_p - E_p \frac{d\phi_p}{dz} = \{U_{s1}/(1-\epsilon_g)\}\phi_p|_{z=H+0}. \qquad (27)$$

They correlated the solid holdup ratio at the exit as follows:

$$\phi_p|_{z=H+0}/\phi_p|_{z=H-0} = 1/\left[1+0.5(v_t/U_g)^{0.4}\right]. \qquad (28)$$

Under their experimental conditions, the ratio was in the range of 1/1.1–1/1.5. Smith and Ruether (1985) reported a fixed value, 1/1.27. They both used glass beads smaller than 200 μm, and the effect of liquid velocity on the solid holdup ratio at the exit was not clearly evaluated. There was no three-phase fluidized-bed zone in their columns, and the local solid holdup decreased exponentially with increasing axial position. When the solid holdup at the exit is small, K_{pr} is calculated from Eqs. 7, 27 and 28 as

$$K_{pr} = \frac{U_1}{(1-\epsilon_g)\left[1+0.5(v_t/U_g)^{0.4}\right]} \frac{\phi_p|_{z=H-0}}{\phi_p|_{z=H+0}}. \qquad (29)$$

Figure 13 shows a comparison between experiment and calculation for the accumulated mass of discharged particles. The particle-size distribution was divided into nine components. Equation 15 gave the best fit, but Eq. 29 was not rejectable.

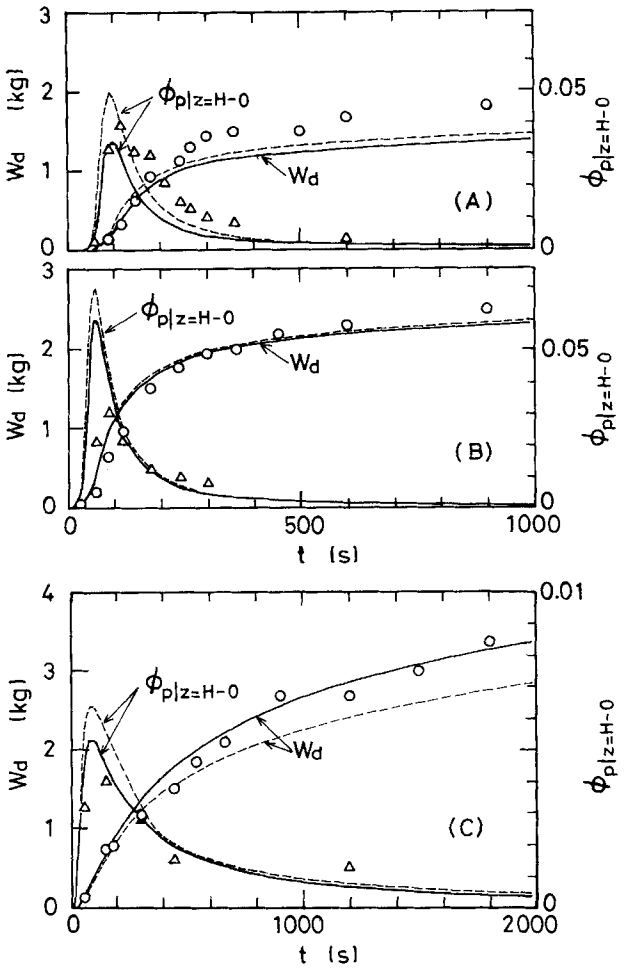

Figure 13. Transient changes in W_d and ϕ_p at $z = H$.

Solid and broken lines are calculated with Eq. 15 and Eq. 29, respectively. Experimental conditions: (A) the same as in Figure 3; (B) the same as in Figure 5; (C) the same as in Figure 6.

The shape of the column exit may change the discharge rate. Figure 14 shows the accumulated mass of discharged particles, W_d, with the side-tube outlet indicated in Figure 1. The data are quite in agreement with the calculation with

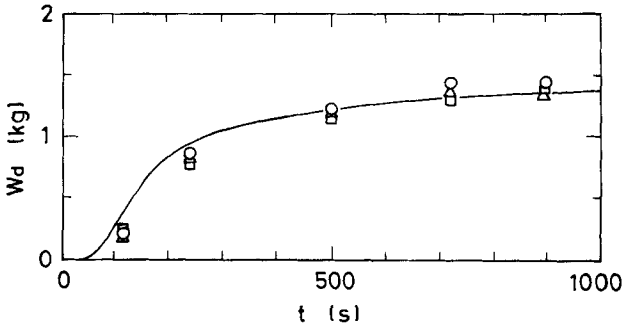

Figure 14. Transient change in mass of solid particles discharged from 7-cm-dia. column installed with side-tube outlet.

Experimental conditions are the same as in Figure 3. Diameter of side-tube outlet: ○, 70 mm; △, 30 mm; □, 12 mm.

K_{pr} correlated by Eq. 15. As indicated in Eq. 8, K_{pr} is a function of $U_1/(1-\epsilon_g)$ and U_{pri}/U_{1r}. The former is intrinsically independent of exit shape. The experimental result shows that the latter is also independent of it. This means that turbulent fluctuations at the exit are somewhat larger than the time-averaged radial velocities, U_{pri} and U_{1r}. Thus the properties of solid particles such as d_{pi} and ρ_p do not affect the value of K_{pr}.

Conclusion

In gas–liquid–solid fluidized systems, the discharge of solid particles from the column top was caused by a step increase in liquid velocity. By stopping the gas and liquid flows simultaneously after a given time period, the mass of discharged particles and the axial distribution of solid holdup in the column were measured. This procedure was repeated, and the transient changes in the flow of solid particles were evaluated. These phenomena were described by an unsteady-state sedimentation-dispersion model, whose parameters were all correlated with empirical equations. Thus the abrupt discharge of solid particles due to an increase in liquid velocity was mathematically described for the first time.

Notation

d_{pi} = diameter of i particle, m
D_T = diameter of column, m
E^*_{pi} = dimensionless axial dispersion coefficient of i particles defined by $E_{pi}/(U_1 H)$
Ga_i = modified Galilei number of i particles defined as $d^3_{pi} g(\rho_p/\rho_1 - 1)/\nu^2$
g = gravitational acceleration, m/s^2
H = height of column, m
k = correction factor defined by Eq. 20
Re_t = Reynolds number defined by $d_p u_t/\nu$
Re_z = Reynolds number defined by $d_p v_z/\nu$
Re^*_1 = Reynolds number defined by $d_{pi}\{\epsilon_g(1-R)(gD_T/2)\}^{1/2}/\nu$
T = dimensionless time defined by tU_1/H
u_{pi} = linear velocity of i particles with respect to fixed coordinate, m/s
u^*_{pi} = dimensionless linear velocity of i particles defined by u_{pi}/U_1
U_{s1} = superficial velocity of slurry, m/s
v_t = terminal settling velocity of a particle in two-phase systems, m/s
v_z = effective settling velocity of solid particles in three-phase systems, m/s
W_{di} = accumulated mass of i particles discharged from outlet, kg
Z = dimensionless axial distance from gas distributor defined by z/H

Greek letters

ν = kinematic viscosity of liquid, m^2/s
ρ_1 = density of liquid, kg/m^3
ρ_p = density of solid particles, kg/m^3
ϕ_{pt} = total solid holdup, $\Sigma\phi_{pi}$

Subscripts

t = total
1 = before change in liquid velocity
2 = after change in liquid velocity

Literature Cited

Al-Dibouni, M. R., and J. Garside, "Particle Mixing and Classification in Liquid Fluidized Beds," *Trans. Inst. Chem. Eng.*, **57**, 94 (1979).

Fan, L.-S., *Gas-Liquid-Solid Fluidization Engineering*, Butterworths, Stoneham, England (1989).

Gosman, A. D., W. A. Pun, A. K. Runchal, D. B. Spalding, and M. Wolfshtein, *Heat and Mass Transfer in Recirculating Flows*, Chap. 3, Academic Press, London (1969).

Hidaka, N., M. Onitani, T. Matsumoto, and S. Morooka, "Axial Mixing and Segregation of Multicomponent Coarse Particles Fluidized by Concurrent Gas-Liquid Flow," *Chem. Eng. Sci.*, **47**, 3427 (1992).

Hidaka, N., T. Masuda, T. Matsumoto, and S. Morooka, "Transient Behavior of the Vertical Distribution of Solid Holdup with a Step Change in Liquid Velocity in a Long Bubble Column," *Ind. Eng. Chem. Res.*, **32**, 1588 (1993).

Imafuku, K., T.-Y. Wang, K. Koide, and H. Kubota, "The Behaviour of Solid Particles in the Bubble Column," *J. Chem. Eng. Japan*, **1**, 153 (1968).

Jiricný, V., and V. Stanék, "Transient of the Hydrodynamics of Counter-Current Packed-Bed Columns," *Chem. Eng. Sci.*, **45**, 449 (1990).

Kato, Y., A. Nishiwaki, T. Fukuda, and S. Tanaka, "The Behavior of Suspended Solid Particles and Liquid in Bubble Columns," *J. Chem. Eng. Japan*, **5**, 112 (1972).

Kato, Y., S. Morooka, T. Kago, T. Saruwatari, and S.-Z. Yang, "Axial Holdup Distributions of Gas and Solid Particles in Three-Phase Fluidized Bed for Gas-Liquid (Slurry)-Solid Systems," *J. Chem. Eng. Japan*, **18**, 308 (1985).

Matsumoto, T., N. Hidaka, and S. Morooka, "Axial Distribution of Solid Holdup in Bubble Column for Gas-Liquid-Solid Systems," *AIChE J.*, **35**, 1701 (1989).

Matsumoto, T., N. Hidaka, H. Takenouchi, and S. Morooka, "Segregation of Solid Particles of Two Sizes in Bubble Columns," *Powder Technol.*, **68**, 131 (1991).

Matsumoto, T., N. Hidaka, H. Gushi, and S. Morooka, "Axial Segregation of Multicomponent Solid Particles Suspended in Bubble Columns," *Ind. Eng. Chem. Res.*, **31**, 1562 (1992).

Morooka, S., T. Mizoguchi, T. Kago, Y. Kato, and N. Hidaka, "Effect of Fine Bubbles on Flow Properties in Bubble Column with Suspended Solid Particles," *J. Chem. Eng. Japan*, **19**, 507 (1986).

Murray, P., and L.-S. Fan, "Axial Solid Distribution in Slurry Bubble Columns," *Ind. Eng. Chem. Res.*, **28**, 1697 (1989).

Richardson, I. F., and W. N. Zaki, "Sedimentation and Fluidization: 1," *Trans. Inst. Chem. Eng.*, **32**, 35 (1954).

Smith, D. N., and J. A. Ruether, "Solid Dynamics in a Slurry Bubble Column," *Chem. Eng. Sci.*, **40**, 741 (1985).

Smith, D. N., J. A. Ruether, Y. T. Shah, and M. N. Badgujar, "Modified Sedimentation-Dispersion Model for Solids in a Three-Phase Slurry Column," *AIChE J.*, **32**, 426 (1986).

Manuscript received May 16, 1994, and revision received Oct. 6, 1994.